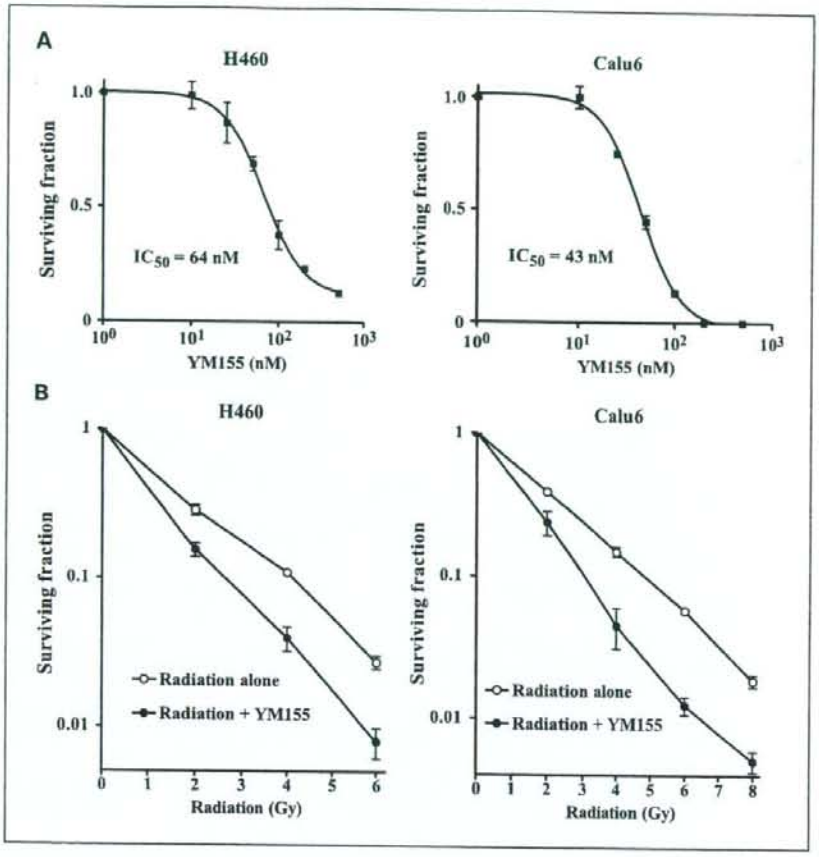

Fig. 2. Effect of YM155 on the sensitivity of H460 or Calu6 cells to γ-radiation. *A*, cells were incubated with the indicated concentrations of YM155 for 48 h and then assayed for clonogenic survival. Points represent means from three independent experiments; bars represent SD. *B*, cells were incubated with 50 nmol/L YM155 or vehicle (control, 0.1% DMSO) for 48 h, exposed to the indicated doses of γ-radiation, and then incubated in drug-free medium for 10 to 14 d for determination of colony-forming ability. Colonies were counted and the surviving fraction was calculated. Plating efficiency for nonirradiated H460 cells was 77.0% and 38.8% for vehicle-treated and YM155-treated cells, respectively; that for nonirradiated Calu6 cells was 57.0% and 23.5%, respectively. All surviving fractions with radiation were corrected for these baseline plating efficiencies. Points represent means from three independent experiments; bars represent SD.

YM155 for up to 72 hours revealed that the abundance of survivin in Calu6 cells had decreased by 2 hours and that survivin was virtually undetectable in H460 cells after 24 hours (Fig. 1B). In both cell lines, treatment with 50 nmol/L YM155 resulted in time-dependent inhibition of survivin expression.

YM155-induced sensitization of NSCLC cells to radiation. To examine the effect of YM155 on cell survival, we first did a clonogenic survival assay. Exposure to the drug at concentrations of 1 to 500 nmol/L for 48 hours revealed that YM155 inhibited the survival of H460 cells with a median inhibitory concentration (IC_{50}) of 64 nmol/L and that of Calu6 cells with an IC_{50} of 43 nmol/L (Fig. 2A). On the basis of these data, we adopted treatment with 50 nmol/L YM155 for 48 hours as the standard protocol for radiation experiments. We next examined whether YM155 might affect the sensitivity of NSCLC cell lines to radiation. Treatment with 50 nmol/L YM155 for 48 hours shifted the survival curves for both H460 and Calu6 cells to the left (Fig. 2B), with a dose enhancement factor of 1.57 and 1.61, respectively, suggesting that YM155 increased the radiosensitivity of both cell lines.

Enhancement of radiation-induced apoptosis in NSCLC cells by YM155. We next examined the effect of YM155 on radiation-induced apoptosis in H460 or Calu6 cells with the use of the TUNEL assay. Combined treatment of either cell line with YM155 and γ-radiation resulted in an increase in the number of apoptotic cells at 24 and 48 hours that was greater than the sum of the increases induced by YM155 or radiation alone (Fig. 3A). To confirm the results of the TUNEL assay, we measured the activity of caspase-3 in cell lysates. Again, the combined treatment of H460 or Calu6 cells with YM155 and γ-radiation induced a synergistic increase in caspase-3 activity (Fig. 3B). These data thus suggested that YM155 promotes radiation-induced apoptosis in NSCLC cell lines.

Inhibition of DNA repair in irradiated NSCLC cells by YM155. Defects in DNA repair have been associated with enhanced sensitivity of cells to radiation (30, 31), and survivin is thought to play a direct or indirect role in DNA repair (21). We therefore next investigated the effect of YM155 on DNA repair by immunostaining of cells with antibodies to the phosphorylated form (γ-H2AX) of histone H2AX, foci of which form at DNA double-strand breaks (DSBs). The formation of γ-H2AX foci in H460 cells was apparent between 30 minutes and 6 hours after γ-irradiation (Fig. 4A). In the presence of YM155, however, these foci persisted for at least 24 hours after irradiation. Evaluation of the percentage of H460 or Calu6 cells with γ-H2AX foci at 24 hours after irradiation revealed that YM155 significantly inhibited the repair of DSBs (Fig. 4B). These results thus suggested that down-regulation of survivin expression by YM155 results in the inhibition of the repair of

radiation-induced DSBs in NSCLC cells, possibly accounting for the observed radiosensitization by this drug.

Enhancement of radiation-induced tumor regression by YM155. To determine whether the YM155-induced radiosensitization of NSCLC cells observed *in vitro* might also be apparent *in vivo*, we injected H460 or Calu6 cells into nude mice to elicit the formation of solid tumors. After tumor formation, the mice were treated with YM155, γ-radiation, or both modalities. YM155 was infused continuously for 7 days with the use of an implanted osmotic pump system, and mice were subjected to local irradiation with a single dose of 10 Gy on day 3 of YM155 administration. Combined treatment with radiation and YM155 inhibited H460 or Calu6 tumor growth to a markedly greater extent than did either modality alone (Fig. 5). The tumor growth delays induced by treatment with radiation alone, YM155 alone, or both YM155 and radiation were 2.9, 5.6, and 14.8 days, respectively, for H460 cells, and 8.9, 41.0, and 76.0 days, respectively, for Calu6 cells. The enhancement factor for the effect of YM155 on the efficacy of radiation was 3.3 for H460 cells and 3.5 for Calu6 cells, revealing the effect to be greater than additive. No pronounced tissue damage or toxicity such as weight loss was observed in mice in any of the four treatment groups.

Finally, we evaluated whether the combination of YM155 and fractionated radiation treatment would result in the inhibition of tumor growth similar to that observed with YM155 plus single-fraction radiation. Mice bearing H460 tumors were thus again subjected to continuous YM155 infusion for 7 days, but local irradiation was done in 2-Gy fractions on days 3 to 7 of drug administration (for a total dose of 10 Gy). The tumor growth delays induced by treatment with radiation alone, YM155 alone, or both YM155 and radiation were 3.8, 5.3, and 16.6 days, respectively (Fig. 6). The enhancement factor for the effect of YM155 on the efficacy of radiation was 3.0. Again, there was no evidence of toxicity on the basis of body weight loss, and there were no animal deaths in any of the four groups. These data suggested that YM155 enhances the tumor response to both single-dose and fractionated radiotherapy *in vivo*.

Discussion

Survivin is a potentially important molecular target for cancer therapy. Reflecting the many mechanisms that seem to regulate survivin expression, diverse approaches have been evaluated for targeting survivin in experimental models. Although certain drugs, such as inhibitors of histone deacetylases,

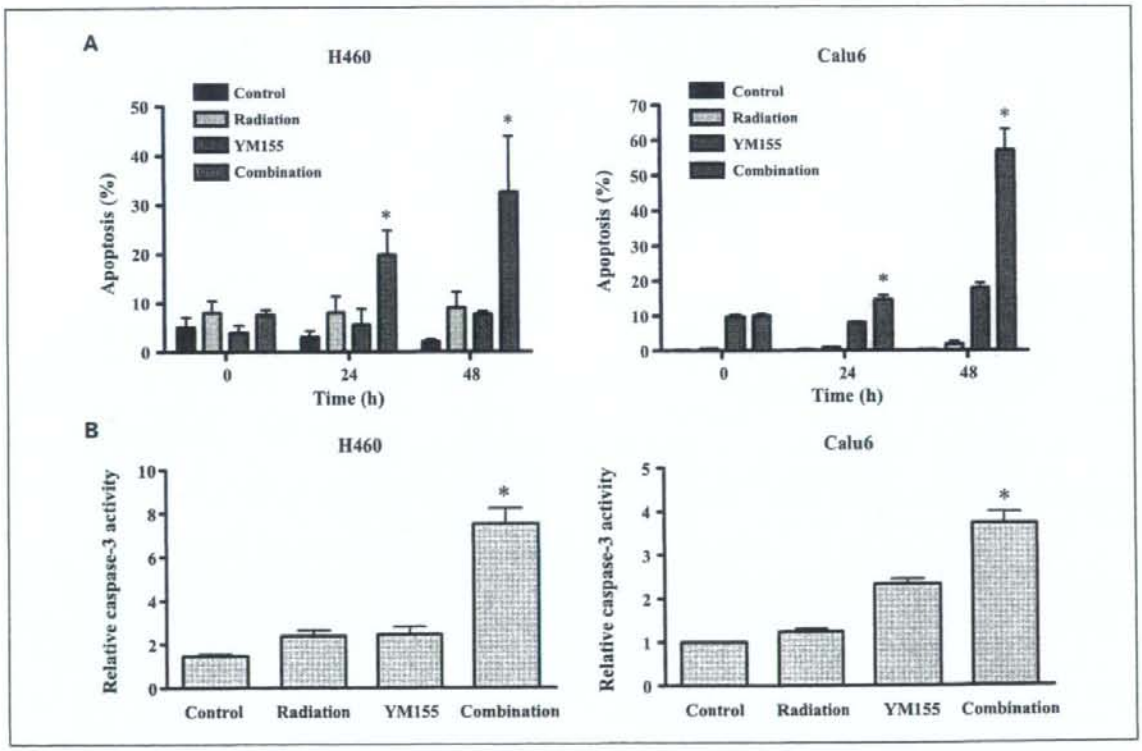

Fig. 3. Effect of YM155 on radiation-induced apoptosis and caspase-3 activity in H460 or Calu6 cells. *A*, cells were incubated with 50 nmol/L YM155 or vehicle (0.1% DMSO) for 48 h, exposed (or not) to 3 Gy of γ-radiation, and then incubated in drug-free medium for 24 or 48 h, at which times the percentage of apoptotic cells was determined by TUNEL staining. *B*, lysates of cells treated as in *A* were assayed for caspase-3 activity 24 h after irradiation. Columns represent means from three independent experiments; bars represent SD; those in *B* are expressed relative to the corresponding value for the control condition. * $P < 0.01$ versus the corresponding value for treatment with radiation or YM155 alone.

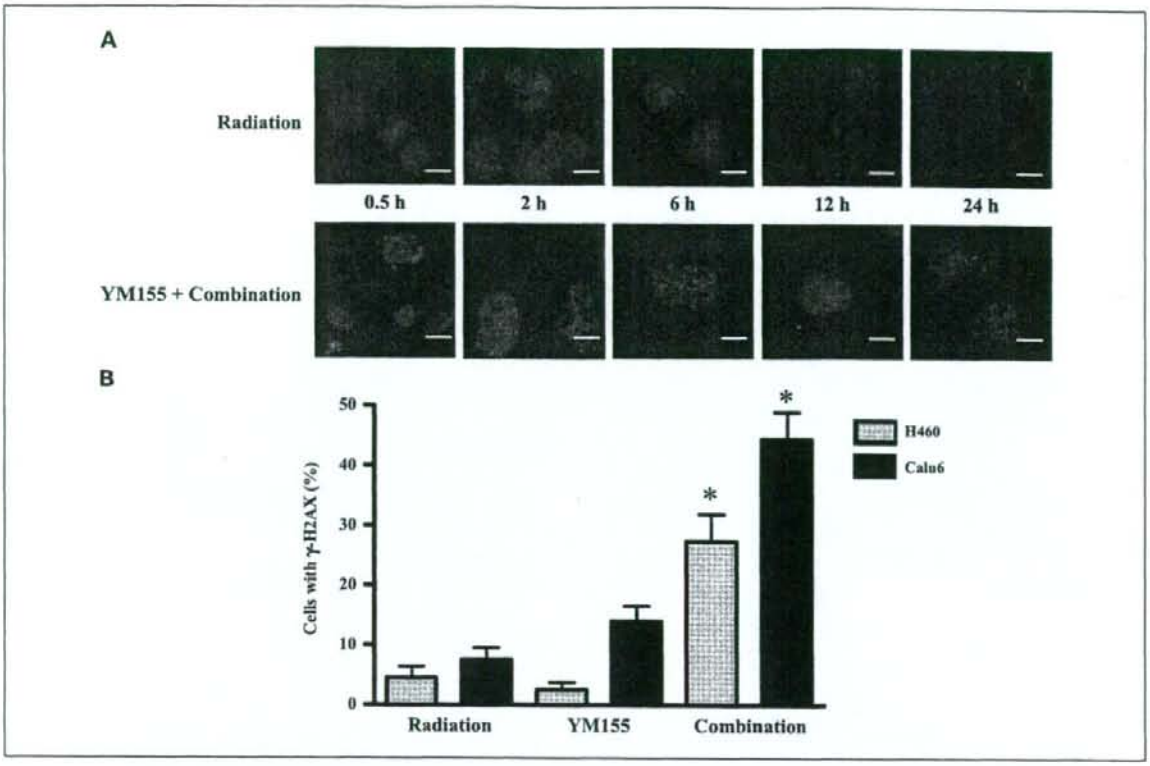

Fig. 4. Effect of YM155 on the radiation-induced formation of γ-H2AX foci in NSCLC cells. *A*, H460 cells were incubated with vehicle (0.1% DMSO) or 50 nmol/L YM155 for 48 h and then exposed to 3 Gy of γ-radiation. After incubation for the indicated times in drug-free medium, the cells were fixed and subjected to immunofluorescence staining for γ-H2AX (green fluorescence). Scale bar, 10 μm. *B*, H460 or Calu6 cells were incubated with vehicle or YM155 and then exposed (or not) to γ-radiation as in *A*. They were fixed at 24 h after irradiation and the percentage of cells containing γ-H2AX foci was determined. Columns represent means from three independent experiments; bars represent SD. $^*P < 0.05$ versus the corresponding value for radiation or YM155 alone.

mitogen-activated protein kinases, and cyclin-dependent kinases, have been shown to suppress survivin expression by targeting various signaling pathways, these drugs inhibit survivin expression nonspecifically (15–17, 19, 32). Gene therapy strategies based on small interfering RNA or other antisense oligonucleotides are specific for survivin, but the effective delivery of these molecules remains a challenge for the transition to the clinic (33). YM155 is a small-molecule agent that specifically inhibits survivin expression in various types of cancer cell lines *in vitro* (14). In addition, YM155 has been shown both to distribute preferentially to tumor tissues rather than to plasma as well as to exert pronounced antitumor activity in tumor xenograft models *in vivo* (14). The use of YM155 as a single agent in phase I clinical trials did not reveal significant toxicity (34). Although phase II studies of YM155 use as a single agent for certain types of cancer are currently under way, the effects of YM155 in combination with radiation have not been reported. We now show that YM155 increased the sensitivity of tumor cells to radiation *in vitro* and *in vivo*.

Clonogenic survival analysis, the most reliable approach for assessing the ability of genotoxic agents to induce cell death (35), revealed that YM155 markedly potentiated the decrease in NSCLC cell survival induced by γ-radiation. Given that induction of apoptosis is a key mechanism of cytotoxicity for most antitumor agents, including γ-radiation, defects in apoptotic signaling may underlie resistance to such agents (36). Radiation-sensitive tumors undergo radiation-induced apoptosis *in vitro* more readily than do radiation-resistant tumors (37–40). Treatment with caspase inhibitors has been shown to protect tumor cells against radiation-induced apoptosis and to increase their radioresistance (21, 41, 42), suggesting that radiation-induced apoptosis is caspase-dependent and that caspases contribute to radiosensitivity. The antiapoptotic activity of survivin is mostly attributable to inhibition of the activation of downstream effectors of apoptosis such as caspase-3 and caspase-7 (25). We have now shown that radiosensitization of NSCLC cells by YM155 was associated with increases both in the activity of caspase-3 and in the proportion of apoptotic cells. Our findings thus suggest that YM155 sensitized tumor cells to radiation at least in part by enhancing radiation-induced apoptosis.

We examined further the mechanism by which YM155 induces radiosensitization. Survivin is essential for the proper execution of mitosis and cell division, with disruption of survivin expression resulting in cell division defects that can lead to polyploidy and the formation of multinucleated cells (43, 44). Although treatment with 50 nmol/L YM155 for 48 hours inhibited survivin expression in NSCLC cells, it

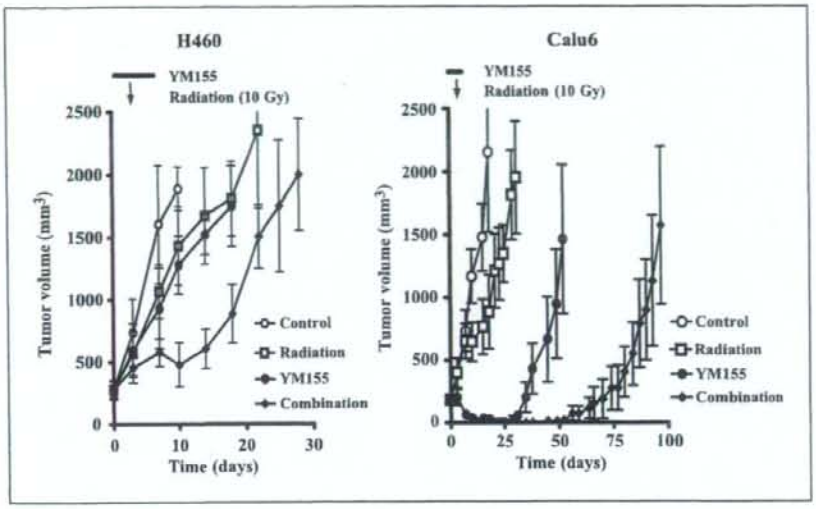

Fig. 5. Effect of YM155 on the growth of H460 or Calu6 tumors in mice subjected to single-dose radiotherapy. Cells were injected into the right hind limb of nude mice and allowed to grow. The mice were divided into four treatment groups: control, radiation alone, YM155 alone, or the combination of YM155 and radiation. YM155 (5 mg/kg) or vehicle was administered by continuous infusion over 7 d, and mice in the radiation groups were subjected to γ-irradiation with a single dose of 10 Gy on day 3 of drug treatment. Tumor volume was measured at the indicated times after the onset of treatment. Points, means from eight mice per group; bars, SE.

did not induce polyploidy (data not shown), suggesting that YM155-induced radiosensitization in the present study was not attributable to cell division defects caused by survivin depletion. Survivin was previously suggested to enhance tumor cell survival after radiation exposure through regulation of DSB repair (21). We therefore investigated the effect of YM155 on the repair of radiation-induced DSBs by immunofluorescence imaging of γ-H2AX foci. H2AX is a histone that is phosphorylated by ataxia telangiectasia mutated and DNA-dependent protein kinase in response to the generation of DSBs (45, 46). This reaction occurs rapidly, with half-maximal amounts of γ-H2AX generated within 1 minute and maximal amounts within 10 minutes (47), and a linear relation has been shown between the number of γ-H2AX foci and that of DSBs (48). The number of γ-H2AX foci is thus a sensitive and specific indicator of the existence of DSBs, with a decrease in this number reflecting DSB repair. We found that YM155 inhibited the repair of radiation-induced DSBs in NSCLC cells. If left unrepaired, DSBs can result in chromosome loss or cell death; agents that inhibit such repair thus increase the sensitivity of cells to ionizing radiation (49, 50). Our results therefore suggest that inhibition of DSB repair by YM155 contributes to the radiosensitization induced by this drug. Given that suppression of survivin expression impairs the repair of radiation-induced DNA damage (9, 21), our results further suggest that inhibition of DNA repair by YM155 is attributable to down-regulation of survivin expression.

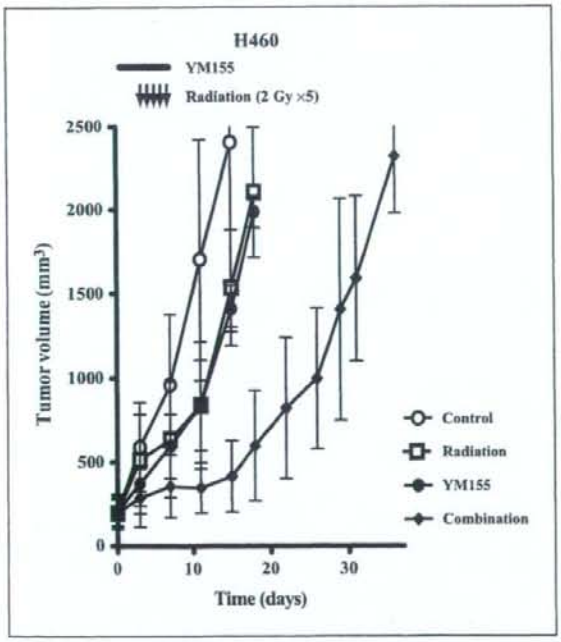

Fig. 6. Effect of YM155 on the growth of H460 tumors in mice subjected to fractionated radiotherapy. H460 cells were injected into the right hind limb of nude mice and allowed to grow. The mice were divided into four treatment groups: control, radiation alone, YM155 alone, or the combination of YM155 and radiation. YM155 (5 mg/kg) or vehicle was administered by continuous infusion over 7 d, and mice in the radiation groups were subjected to γ-irradiation with a daily dose of 2 Gy on days 3 to 7 of drug treatment. Tumor volume was measured at the indicated times after the onset of treatment. Points represent means from eight mice per group; bars represent SE.

The antitumor activity of YM155 has previously been shown to be time-dependent, with continuous infusion of the drug resulting in greater antitumor activity and less systemic toxicity compared with bolus injection in tumor xenograft models *in vivo* (14). Ongoing clinical trials of YM155 are thus being done with the drug administered on a continuous schedule. We also administered YM155 by continuous infusion in our *in vivo* experiments. The combination of YM155 with single-dose radiotherapy resulted in a marked increase in tumor growth delay compared with that apparent with either radiation or YM155 alone, indicating that YM155 enhanced the antitumor effect of ionizing radiation *in vivo*. Given that standard radiation therapy in the clinic is delivered according to a fractionated schedule, we also examined whether YM155 enhanced the tumor response to clinically relevant fractionated doses (2 Gy) of radiation. Indeed, YM155 was also effective in

Pharmacokinetic Analysis of Carboplatin and Etoposide in a Small Cell Lung Cancer Patient Undergoing Hemodialysis

Ken Takezawa, MD, Isamu Okamoto, MD, PhD, Masahiro Fukuoka, MD, PhD, and Kazuhiko Nakagawa, MD, PhD

Cancer chemotherapy is not well established for patients on hemodialysis (HD). A 77-year-old man on HD presented with small cell lung cancer. He was treated with the combination of carboplatin and etoposide while the pharmacokinetics of the drugs were monitored. The patient showed a response with manageable toxicity and remained progression free for at least 8 months. The area under the concentration-time curve for each antitumor agent in the patient was within the therapeutic range achieved in individuals with normal renal function. Carboplatin and etoposide chemotherapy combined with HD thus allowed the drugs to achieve an appropriate area under the concentration-time curve and sufficient efficacy in a small cell lung cancer patient with chronic renal failure.

Key Words: Small cell lung cancer, Hemodialysis, Pharmacokinetics, Chemotherapy.

(*J Thorac Oncol.* 2008;3: 1073–1075)

The prognosis of patients with chronic renal failure has improved as a result of progress in hemodialysis (HD), and opportunities to treat malignant tumors that develop in such HD patients are increasing. However, little is known of the safety or efficacy of chemotherapy for malignant tumors in HD patients. We analyzed the pharmacokinetics of combination chemotherapy with carboplatin (CBDCA) and etoposide in a patient with small cell lung cancer (SCLC) undergoing HD.

CASE REPORT

A 77-year-old man with chronic renal failure due to diabetic nephropathy presented with a mass in the left hilar area in March 2007. The general condition of the patient, who had undergone HD, three times a week, was fair, with symptoms such as cough, weight loss, and fever being absent. His Eastern Cooperative Oncology Group performance status was 1. Computed tomography of the chest revealed a 45/33 mm mass in the lower left lobe as well as interstitial pneumonia in the lower left and lower right lobes. Histopathologic analysis of a transbronchial biopsy specimen revealed SCLC. No distant metastasis was detected on systemic examinations, and the patient was diagnosed with limited-stage SCLC. Laboratory testing revealed blood urea nitrogen and creatinine levels of 101 and 8.6 mg/dl, respectively. Other examined laboratory parameters were within normal limits, but subsequent evaluation of serum tumor markers revealed an increased level (18.2 ng/ml) of neuron-specific enolase, which is not affected by renal function.[1]

Radiotherapy was not appropriate for the patient because of his bilateral interstitial pneumonia. Given his good performance status and after obtaining informed consent, we treated the patient with the combination of CBDCA and etoposide (Figure 1). On day 1 of the treatment cycle, the patient received an intravenous injection of etoposide (50 mg/m^2) over 60 minutes followed by an intravenous injection of CBDCA (250–275 mg/m^2) also over 60 minutes. HD was initiated 60 minutes after completion of CBDCA administration and was performed for 4 hours. On day 3, etoposide (50 mg/m^2) was administered over 60 minutes and HD was performed for 4 hours beginning 2 hours after completion of etoposide injection. The doses of CBDCA and etoposide as well as the timing of HD were based on previous studies.[2–4] The treatment was well tolerated. Nonhematologic toxicities such as nausea, vomiting, and fatigue were not observed. The patient also did not experience neutoropenia or thrombocytopenia (Nadir neutrophil and platelet counts during 3 cycles of chemotherapy were 2200/μl and 15.5 $\times$ 10^4/μl, respectively). Prophylactic administration of granulocyte colony-stimulating was not carried out. After three cycles of chemotherapy, each separated by an interval of 3 weeks, the tumor had decreased in size and the serum neuron-specific enolase level had decreased to within normal limits (6.3 ng/ml). The patient remained progression free 8 months after the initiation of treatment.

Pharmacokinetic analysis of CBDCA and etoposide was performed for the first and third courses of chemotherapy. Serial blood samples were collected 0, 1, 2, 3, 4, 5, 6, 24, 37, 41, 42, 49, 53, and 54 hours after completion of CBDCA administration as well as 0, 2, 3, 4, 5, 6, 7, 25, 48, 50, 52, 54, 55, and 73 hours after completion of the first etoposide administration. Each blood sample was analyzed for free

Department of Medical Oncology, Kinki University School of Medicine, Osaka, Japan.

Disclosure: The authors declare no conflicts of interest.

Address for correspondence: Isamu Okamoto, MD, PhD, Department of Medical Oncology, Kinki University School of Medicine, 377-2 Ohno-higashi, Osaka-Sayama, Osaka 589-8511, Japan. E-mail: chi-okamoto@dotd.med.kindai.ac.jp

ISSN: 1556-0864/08/0309-1073

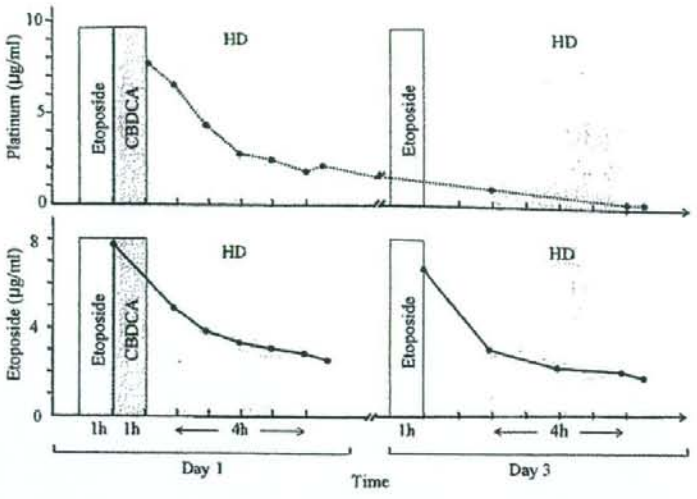

FIGURE 1. Chemotherapy and hemodialysis schedule as well as the plasma concentrations of free platinum and etoposide for the proband. Data are for the first of three cycles of chemotherapy. HD, hemodialysis; CBDCA, carboplatin.

platinum and etoposide (Figure 1) as described previously.[5] In the first cycle, the area under the concentration-time curve (AUC) was 4.10 minutes mg/ml for free platinum and 4401 and 3612 minutes μg/ml for etoposide on days 1 and 3, respectively. In the third course of chemotherapy, for which the CBDCA dose was increased from 250 to 275 mg/m^2, the AUC of free platinum was 4.16 minutes mg/ml. The maximal concentration and half-life of free platinum were 7.7 μg/ml and 2.51 hours in the first cycle and 9.4 μg/ml and 1.93 hours in the third cycle.

DISCUSSION

Many lung cancer patients undergoing HD as a result of impaired renal function may be "undertreated" because chemotherapy regimens are not well established for such individuals. The lack of pharmacokinetic data for most cytotoxic agents in HD patients makes it difficult to administer chemotherapy effectively. Given his old age, bilateral interstitial pneumonia, and renal dysfunction, the present patient might have been considered too high a risk for chemotherapy and recommended to receive best supportive care. However, taking into account the sensitivity of SCLC to platinum combination chemotherapy, we treated him with CBDCA and etoposide while monitoring the pharmacokinetics of these antitumor agents.

CBDCA is a less emetic and less nephrotoxic analog of cisplatin and is preferred over cisplatin for use in patients with renal insufficiency. The desired AUC for CBDCA can be individualized with the use of Calvert's formula on the basis of individual renal function.[6] In previous studies of CBDCA-based chemotherapy in patients undergoing HD, a CBDCA dose of 100 to 150 mg/body was chosen according to this formula, with the glomerular filtration rate set to zero because of the absence of renal function (Table 1).[7–10] In these studies, HD was performed 16 to 24 hours after completion of CBDCA administration, resulting in an AUC of 4.43 to 6.9 minutes mg/ml. More recently, administration of a relatively high dose (300 mg/m^2) of CBDCA with initiation of HD 0.5 to 1.5 hours after completion of drug injection has been shown to be feasible and effective in lung cancer patients undergoing HD.[2–4] However, the AUC of CBDCA in these latter studies was not determined. In the present study, we found that a CBDCA dose of 250 to 275 mg/m^2 administered completely 1 hour before HD gave rise to an AUC for free platinum of 4.10 to 4.16 minutes mg/ml, a therapeutic blood level, consistent with the antitumor efficacy observed

TABLE 1. Previous Studies of Carboplatin-Based Chemotherapy in Cancer Patients on Hemodialysis

	Disease	No. of Patients	Carboplatin Dose	Interval Between Carboplatin Infusion and Hemodialysis (h)	AUC (min mg/ml)
Watanabe et al.[7]	Ovarian cancer	1	125 mg	16	4.43
Jeyabalan et al.[8]	Ovarian cancer	1	125 mg	24	N.D
Chatelut et al.[9]	Ovarian cancer	1	150 mg	24	6.06–6.70
Motzer et al.[10]	Germ cell tumor	2	100 mg/m^2	24	6.7–6.9
Inoue et al.[2]	SCLC	3	300 mg/m^2	1	N.D
Yanagawa et al.[3]	NSCLC/epipharynx ca	2	300 mg/m^2	0.5	N.D
Haraguchi et al.[4]	SCLC	1	300 mg/m^2	1.5	N.D

N.D, not determined; NSCLC, non-small cell lung cancer.

in the previous studies[2–4]. Our presented study supports that relatively high dose administration of CBDCA with initiation of HD 1 hour after drug injection would be an alternative strategy for patients with HD -dependent renal insufficiency.

Etoposide is active against various types of malignant tumors, but its membrane permeability in HD remains unclear. The AUC range for etoposide in 13 patients with normal renal function treated with this drug at a dose of 100 mg/m^2 was previously shown to be 2291 to 6832 minutes μg/ml (Ref. [11]). The present patient was treated with etoposide at 50 mg/m^2 on days 1 and 3, with HD being initiated 2 hours after completion of the drug injection. The AUC of etoposide was 3612 to 4401 minutes μg/ ml, values that are within the range achieved in patients with normal renal function. Indeed, the combination chemotherapy in the proband induced a tumor response that persisted for at least 8 months. Administration of etoposide at 100 mg/m^2 on days 1, 3, and 5 in combination with cisplatin at 80 mg/m^2 was shown to be acceptable in 4 lung cancer patients with renal dysfunction.[12] In the previous study, HD was performed soon after drug administration, resulting in an AUC for etoposide of 4800 to 6204 minutes μg/ml. Data from the previous studies and our present patient thus indicate that etoposide can be administered safely in HD patients.

The present case shows that CBDCA and etoposide chemotherapy combined with HD resulted in AUCs for these drugs within the therapeutic range in a SCLC patient with chronic renal failure. Although further studies are needed, our findings suggest that this regimen of combination chemotherapy can be administered to lung cancer patients with renal insufficiency.

REFERENCES

1. Xiaofang Y, Yue Z, Xialian X, et al. Serum tumour markers in patients with chronic kidney disease. *Scand J Clin Lab Invest* 2007;67:661–667.
2. Inoue A, Saijo Y, Kikuchi T, et al. Pharmacokinetic analysis of combination chemotherapy with carboplatin and etoposide in small-cell lung cancer patients undergoing hemodialysis. *Ann Oncol* 2004;15:51–54.
3. Yanagawa H, Takishita Y, Bando H, et al. Carboplatin-based chemotherapy in patients undergoing hemodialysis. *Anticancer Res* 1996;16: 533–535.
4. Haraguchi N, Satoh H, Ogawa R, et al. Chemotherapy in a patient with small-cell lung cancer undergoing hemodialysis. *Clin Oncol* 2005;17: 663–668.
5. LeRoy AF, Wehling ML, Sponseller HL, et al. Analysis of platinum in biological materials by flameless atomic absorption spectrophotometry. *Biochem Med* 1977;18:184–191.
6. Calvert AH, Newell DR, Gumbrell LA, et al. Carboplatin dosage: prospective evaluation of a simple formula based on renal function. *J Clin Oncol* 1989;7:1748–1756.
7. Watanabe M, Aoki Y, Tomita M, et al. Paclitaxel and carboplatin combination chemotherapy in a hemodialysis patient with advanced ovarian cancer. *Gynecol Oncol* 2002;84:335–338.
8. Jeyabalan N, Hirte HW, Moens F. Treatment of advanced ovarian carcinoma with carboplatin and paclitaxel in a patient with renal failure. *Int J Gynecol Cancer* 2000;10:463–468.
9. Chatelut E, Rostaing L, Gualano V, et al. Pharmacokinetics of carboplatin in a patient suffering from advanced ovarian carcinoma with hemodialysis-dependent renal insufficiency. *Nephron* 1994;66:157–161.
10. Motzer RJ, Niedzwiecki D, Isaacs M, et al. Carboplatin-based chemotherapy with pharmacokinetic analysis for patients with hemodialysis-dependent renal insufficiency. *Cancer Chemother Pharmacol* 1990;27: 234–238.
11. D'Incalci M, Farina P, Sessa C, et al. Pharmacokinetics of VP16–213 given by different administration methods. *Cancer Chemother Pharmacol* 1982;7:141–145.
12. Watanabe R, Takiguchi Y, Moriya T, et al. Feasibility of combination chemotherapy with cisplatin and etoposide for haemodialysis patients with lung cancer. *Br J Cancer* 2003;88:25–30.

FEBS Letters 582 (2008) 4125–4130

The anti-EGFR monoclonal antibody blocks cisplatin-induced activation of EGFR signaling mediated by HB-EGF

Takeshi Yoshida[a], Isamu Okamoto[a,*], Tsutomu Iwasa[a], Masahiro Fukuoka[b], Kazuhiko Nakagawa[a]

[a] Department of Medical Oncology, Kinki University School of Medicine, 377-2 Ohno-higashi, Osaka-Sayama, Osaka 589-8511, Japan
[b] Kinki University School of Medicine, Sakai Hospital, 2-7-1 Harayamadai, Minami-ku Sakai, Osaka 590-0132, Japan

Received 21 July 2008; revised 2 October 2008; accepted 11 November 2008

Available online 21 November 2008

Edited by Richard Marais

Abstract **Cisplatin is a key agent in combination chemotherapy for various types of solid tumor. We now show that cisplatin activates signaling by the epidermal growth factor receptor (EGFR) by inducing cleavage of heparin-binding epidermal growth factor-like growth factor (HB-EGF). Matuzumab, a monoclonal antibody to EGFR, inhibited cisplatin-induced EGFR signaling, likely through competition with the soluble form of HB-EGF for binding to EGFR. Matuzumab enhanced the antitumor effect of cisplatin in nude mice harboring human non-small cell lung cancer xenografts. Our findings shed light on the mechanism by which monoclonal antibodies to EGFR might augment the efficacy of cisplatin.**

Keywords: EGF receptor; Heparin-binding EGF-like growth factor; Matuzumab; Cisplatin; Non-small cell lung cancer

1. Introduction

Cisplatin is a key component of combination chemotherapy for various types of solid tumor, but its effectiveness is limited by the development of chemoresistance [1]. Several nonphysiological stimuli that induce cellular stress, such as hyperosmolarity, wounding, UV or γ-radiation, reactive oxygen species, and chemotherapeutic agents, trigger activation of the epidermal growth factor receptor (EGFR) [2–11]. Ligand binding to EGFR induces receptor dimerization and activation of the receptor kinase, triggering intracellular signaling pathways such as those mediated by the protein kinases Akt or extracellular signal-regulated kinase (Erk), which play fundamental roles in the control of numerous cellular processes such as growth, proliferation, and survival [12–18]. EGFR signaling pathways activated by cellular stressors are thus of clinical interest because of their potential role in tumor resistance to chemotherapy [2–11]. The effects of cisplatin on EGFR signaling pathways have remained unclear, but the potential role of these pathways in cisplatin resistance makes it important to examine whether EGFR inhibitors might enhance the antitumor effects of this drug [8,9].

We have now examined the molecular mechanism of cisplatin-induced activation of EGFR and the effects of this drug on downstream signaling pathways. We also examined the effects of matuzumab (EMD72000, humanized mouse immunoglobulin G1), a monoclonal antibody (mAb) to EGFR [19], on cisplatin-dependent EGFR signaling. Finally, the antitumor effect of matuzumab combined with cisplatin was evaluated in order to provide insight into the mechanism by which anti-EGFR mAbs might augment the efficacy of cisplatin.

2. Materials and methods

2.1. Cell culture and reagents

The human non-small cell lung cancer (NSCLC) cell lines NCI-H292 (H292), NCI-H460 (H460), and A549 were obtained and cultured as previously described [20]. Matuzumab and gefitinib were also obtained as previously described [19]; GM6001 was from Calbiochem (La Jolla, CA); cisplatin, CRM197, and epidermal growth factor (EGF) were from Sigma (St. Louis, MO); and heparin-binding EGF-like growth factor (HB-EGF) was from R&D Systems (Minneapolis, MN).

2.2. Immunoblot analysis

Immunoblot analysis was performed as described previously [20]. Primary antibodies to the Tyr^{845}-phosphorylated form of EGFR, to EGFR, to phosphorylated Erk, to Erk, to phosphorylated Akt, and to Akt as well as horseradish peroxidase (HRP)-conjugated goat antibodies to mouse or rabbit immunoglobulin G were obtained as described previously [20]. Primary antibodies to the intracellular COOH-terminal domain of HB-EGF and HRP-conjugated donkey antibodies to goat immunoglobulin G were from Santa Cruz Biotechnology (Santa Cruz, CA).

2.3. Assessment of tumor growth inhibition in vivo

Tumor cells (2×10^6) were injected subcutaneously into the flank of 7-week-old female athymic nude mice. The mice were divided into four treatment groups of seven or eight animals: those treated over 2 weeks by intraperitoneal injection of vehicle, matuzumab (0.05 mg, twice per week), cisplatin (6 mg/kg of body weight, twice per week), or both matuzumab and cisplatin. Treatment was initiated when tumors in each group achieved an average volume of 200 mm^3, with tumor volume being determined twice weekly for 41 days after the onset of treatment from caliper measurement of tumor length (L) and width (W) according to the formula $LW^2/2$.

2.4. Ki67 index

Tumors were removed from some animals 14 days after treatment initiation and were stained with a mouse mAb to human Ki67 (clone MIB-1; Dako, Carpinteria, CA), as previously described [21]. The

*Corresponding author. Fax: +81 72 360 5000.
E-mail address: chi-okamoto@dotd.med.kindai.ac.jp (I. Okamoto).

Abbreviations: EGF, epidermal growth factor; EGFR, EGF receptor; mAb, monoclonal antibody; NSCLC, non-small cell lung cancer; HB-EGF, heparin-binding EGF-like growth factor; HRP, horseradish peroxidase; TUNEL, terminal deoxynucleotidyl transferase-mediated dUTP nick-end labeling

0014-5793/$34.00
doi:10.1016/j.febslet.2008.11.010

Ki67 index was determined as the percentage of Ki67-positive cells by scoring at least 300 tumor cells in each of 10 well-preserved fields of each tumor at a magnification of ×200 (CX41 light microscope; Olympus, Tokyo, Japan).

2.5. TUNEL staining

Terminal deoxynucleotidyl transferase-mediated dUTP nick-end labeling (TUNEL) analysis of tumor sections was performed as described previously [22]. The number of apoptotic cells in each of 10 fields (×200) per tumor was determined with a light microscope (CX41, Olympus).

2.6. Statistical analysis

Quantitative data are presented as means ± S.D. and were compared among groups by one-way analysis of variance followed by Tukey's multiple comparison test. A P value of <0.05 was considered

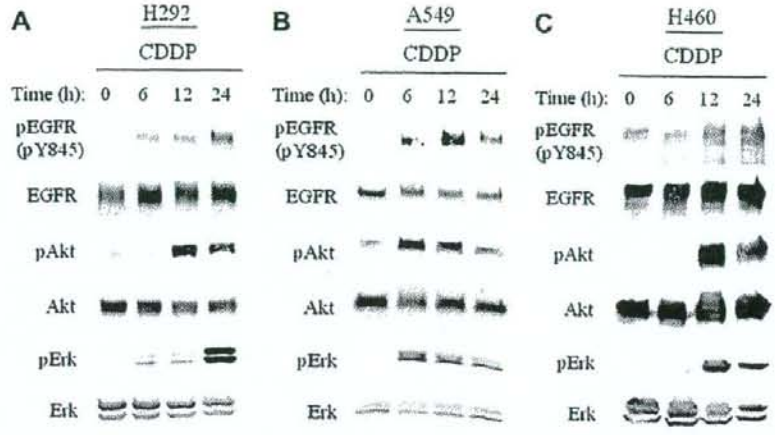

Fig. 1. Cisplatin-induced activation of EGFR and of downstream signaling pathways mediated by Akt or Erk. Serum-deprived H292 (A), A549 (B), or H460 (C) cells were incubated for the indicated times in the absence or presence of cisplatin (CDDP, 100 μM). Cell lysates were then subjected to immunoblot analysis with antibodies to the Tyr^{845}-phosphorylated form of EGFR (pEGFR), to phosphorylated Akt, or to phosphorylated Erk as well as with antibodies to total forms of these proteins.

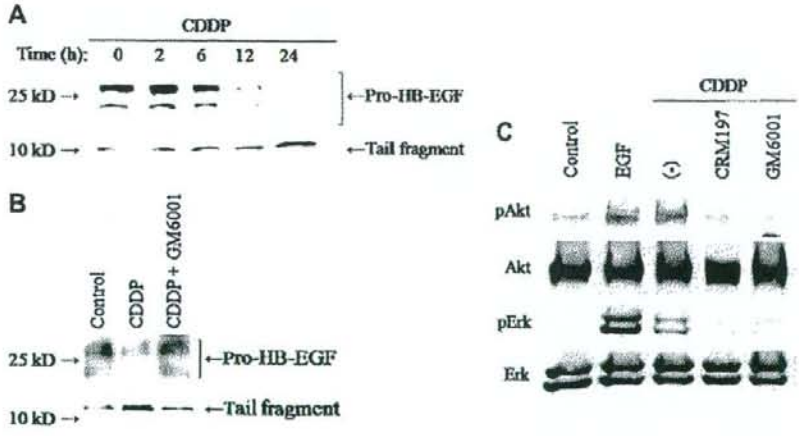

Fig. 2. Cisplatin-induced HB-EGF cleavage and its role in activation of EGFR signaling pathways by cisplatin. (A) Serum-deprived H292 cells were incubated for the indicated times in the presence of cisplatin (100 μM). Cell lysates were then subjected to immunoblot analysis with antibodies to the intracellular COOH-terminal domain of HB-EGF. The positions of molecular size standards (left) as well as of bands corresponding to pro-HB-EGF and to the cleaved tail fragment (right) are indicated. (B) Serum-deprived H292 cells were incubated alone (control) or with cisplatin (100 μM) in the absence or presence of GM6001 (10 μM) for 12 h. Cell lysates were then subjected to immunoblot analysis as in (A). (C) Serum-deprived H292 cells were incubated with EGF (100 ng/ml) for 15 min as a positive control or with cisplatin (100 μM) in the absence or presence of GM6001 (10 μM) or CRM197 (10 μg/ml) for 12 h. Cell lysates were then subjected to immunoblot analysis with antibodies to phosphorylated or total forms of Akt or Erk.

statistically significant. Statistical analysis was performed with GraphPad Prism version 5.00 for Windows (GraphPad Software, San Diego, CA).

3. Results and discussion

3.1. Cisplatin activates EGFR as well as downstream Akt and Erk signaling pathways

Cellular stress induced by several chemotherapeutic agents or γ-radiation triggers the activation of EGFR signaling pathways, with this effect being thought to play an important role in resistance to chemotherapy or radiotherapy [6–11]. We examined the effects of cisplatin on EGFR and downstream signaling pathways mediated by Akt or Erk in human NSCLC cell lines (H292, A549, H460). Cisplatin induced the phosphorylation of EGFR, Akt, and Erk in a time-dependent manner, without affecting the total amounts of these proteins, in all three cell lines (Fig. 1). These results thus showed that cisplatin activates EGFR and downstream signaling pathways mediated by Akt or Erk.

3.2. Cisplatin activates EGFR signaling pathways by inducing the cleavage of HB-EGF

HB-EGF is a membrane-bound EGFR ligand that activates EGFR after its release from the membrane in response to cellular stress [3,5,23–25]. To determine whether HB-EGF contributes to cisplatin-induced EGFR signaling, we examined the possible effect of cisplatin on cleavage of the membrane-bound pro-form of HB-EGF in H292 cells. Cisplatin induced a time-dependent decrease in the amount of pro-HB-EGF and a consequent increase in the amount of a COOH-terminal fragment of this protein referred to as the "tail fragment" (Fig. 2A). These effects of cisplatin were inhibited by GM6001 (Fig. 2B), a potent inhibitor of matrix metalloproteinases responsible for HB-EGF cleavage [23,24], suggesting that cisplatin induces metalloproteinase-mediated cleavage of the ectodomain of HB-EGF and its release from the cell sur-

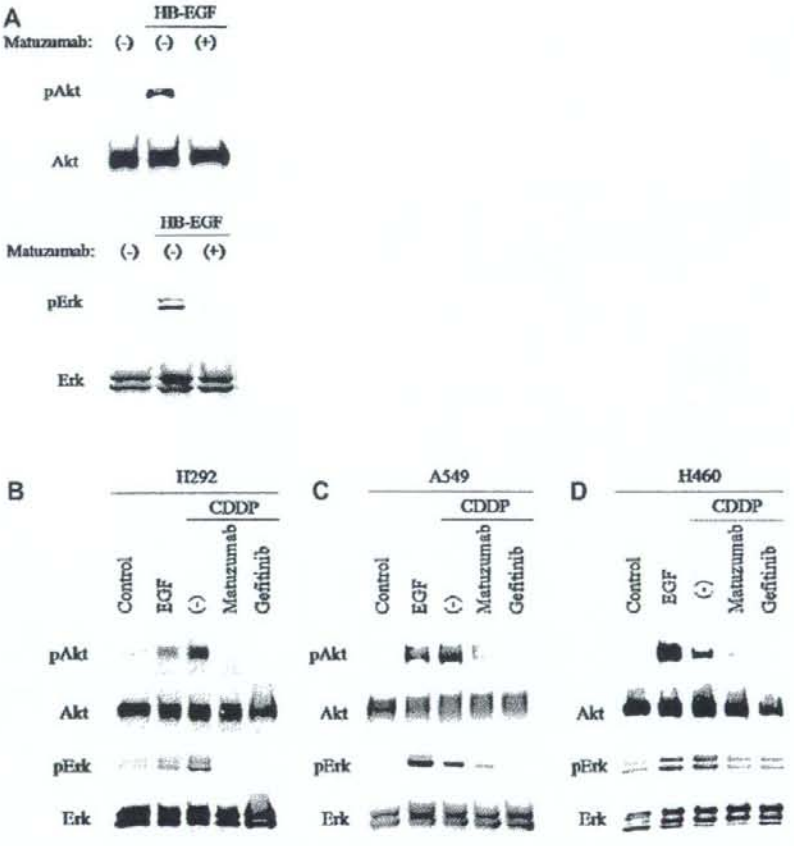

Fig. 3. Inhibition by matuzumab of EGFR signaling induced by HB-EGF or by cisplatin. (A) Serum-deprived H292 cells were incubated first for 2 h in the absence or presence of matuzumab (200 nM) and then for 15 min in the additional absence or presence of HB-EGF (10 ng/ml). Cell lysates were then subjected to immunoblot analysis with antibodies to phosphorylated or total forms of Akt or Erk. (B–D) Serum-deprived H292 (B), A549 (C), or H460 (D) cells were incubated with EGF (100 ng/ml) for 15 min as a positive control or with cisplatin (100 μM) in the absence or presence of matuzumab (200 nM) or gefitinib (10 μM) for 12 h. Cell lysates were then subjected to immunoblot analysis as in (A).

face. GM6001 also blocked the activation of Akt and Erk by cisplatin (Fig. 2C), implicating HB-EGF cleavage in cisplatin-induced EGFR signaling. To explore further whether cisplatin-induced EGFR signaling is dependent on HB-EGF activity, we examined the effect of CRM197, a nontoxic mutant form of diphtheria toxin that binds specifically to and neutralizes HB-EGF, which has also been identified as a diphtheria toxin receptor [26]. CRM197 completely inhibited the activation of Akt and Erk by cisplatin (Fig. 2C), suggesting that cisplatin promotes EGFR signaling by inducing the cleavage of HB-EGF. Consistent with this notion, the time course of cisplatin-induced activation of EGFR signaling (Fig. 1A) was similar to that of cisplatin-induced release of HB-EGF from the cell surface (Fig. 2A).

Cisplatin has previously been shown to increase the amount of HB-EGF mRNA in various types of cancer cells [7], and expression of the HB-EGF gene was found to be increased in cisplatin-resistant cancer [27]. The chemotherapeutic drugs SN38, doxorubicin, and imatinib also induce EGFR signaling and subsequent chemoresistance through metalloproteinase-dependent cleavage of HB-EGF [7,10]. It is possible that EGFR signaling resulting from metalloproteinase-mediated cleavage of HB-EGF represents a common mechanism of cellular resistance to various chemotherapeutic agents.

3.3. Effects of matuzumab on cisplatin-induced EGFR signaling

The clinical efficacy of treatment with anti-EGFR mAbs has been thought to be due to their prevention of ligand binding to EGFR [28,29]. We hypothesized that anti-EGFR mAbs might inhibit cisplatin-induced EGFR signaling by blocking the binding of the released ectodomain of HB-EGF to EGFR. To test whether anti-EGFR mAbs inhibit EGFR signaling induced by HB-EGF, we examined the effects of the humanized anti-EGFR mAb matuzumab. Matuzumab indeed prevented the activation of Akt and Erk by HB-EGF (Fig. 3A), indicating that this mAb inhibits HB-EGF–dependent EGFR signaling. We next examined the effect of matuzumab on cisplatin-induced EGFR signal transduction. The activation of EGFR downstream signaling by cisplatin was abolished by gefitinib in H292, A549, and H460 cells (Fig. 3B–D), suggesting that cisplatin-induced EGFR signaling requires the tyrosine kinase activity of EGFR. Matuzumab also markedly inhibited

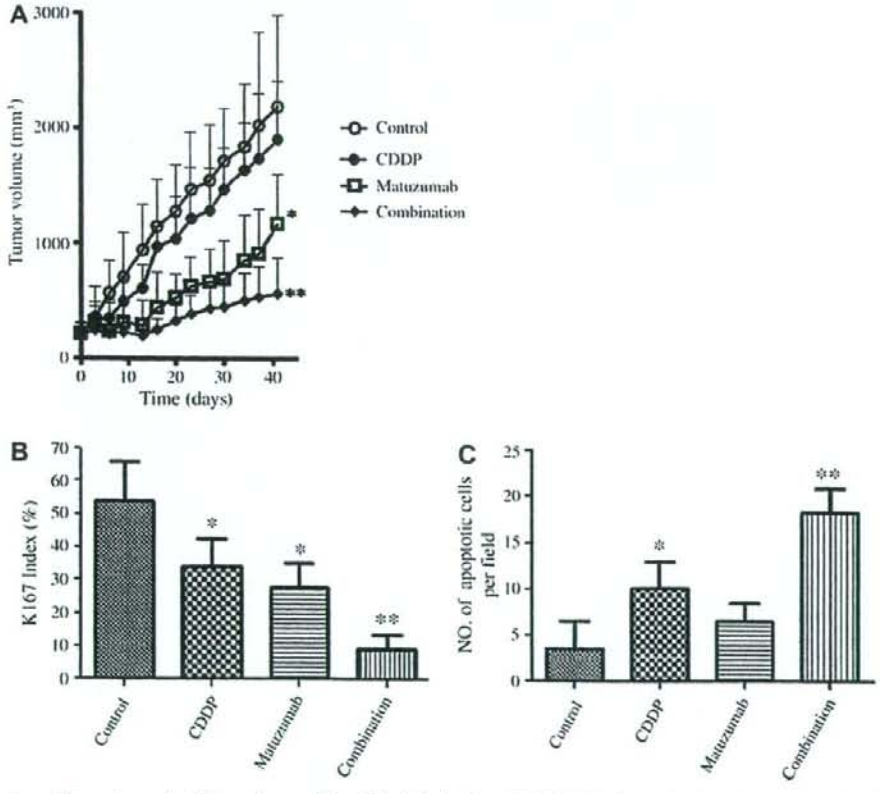

Fig. 4. Enhancement by matuzumab of the antitumor effect of cisplatin in vivo. (A) Nude mice harboring H292 tumor xenografts (200 mm³) were treated with a single intraperitoneal dose of matuzumab (0.05 mg) or cisplatin (6 mg/kg), with both agents, or with vehicle (control) twice a week for 14 days. Tumor volume was determined at the indicated times after the onset of treatment. (B) The Ki67 index was determined from sections of H292 tumor xenografts 14 days after the initiation of treatment as in (A). (C) Quantitation by TUNEL staining of the number of apoptotic cells per field (×200) in H292 tumor xenografts 14 days after the initiation of treatment as in (A). Data in (A–C) are means ± S.D. $^{*}P < 0.05$ versus control; $^{**}P < 0.05$ versus control or each agent alone.

cisplatin-induced EGFR signaling in all three cell lines (Fig. 3B–D). These results thus suggested that matuzumab blocks cisplatin-induced EGFR signaling through inhibition of HB-EGF-dependent activation of EGFR.

Matuzumab exerts its antitumor effect both by competition with EGF for binding to EGFR and by blockade of the EGFR turnover that is important for activation of downstream signaling pathways mediated by Akt or Erk [19,28,29]. The soluble form of HB-EGF includes the EGF-like domain, a common structure in members of the EGF family of proteins that consists of 40–45 amino acids and contains six cysteine residues, but it binds not only to EGFR but also to ErbB4, whereas EGF binds specifically to EGFR [23–25]. The corresponding binding site of EGFR or the ligand function of HB-EGF may therefore differ from those for EGF. Nevertheless, we have now shown that matuzumab also inhibits the activation of EGFR signaling by both HB-EGF and cisplatin.

3.4. Matuzumab enhances the antitumor action of cisplatin in H292 xenografts

If cisplatin-induced EGFR signaling plays an important role in the development of cisplatin resistance, matuzumab might be expected to enhance the antitumor effect of cisplatin by inhibiting such signaling. We therefore determined the efficacy of combined treatment with matuzumab and cisplatin in nude mice with solid tumors formed by H292 cells injected into the flank. Combination therapy with matuzumab and cisplatin inhibited tumor growth to a significantly greater extent than did treatment with matuzumab or cisplatin alone (Fig. 4A).

Tumors treated with the combination of matuzumab and cisplatin also manifested both a significantly smaller Ki67 index (Fig. 4B), a marker of cell proliferation, and a significantly greater proportion of apoptotic cells (Fig. 4C), compared with tumors treated with either agent alone. Matuzumab alone or in combination with cytotoxic agents was previously shown to inhibit Akt or Erk phosphorylation in human tissue samples or human xenografts in nude mice [30–34]. The combination of matuzumab and cisplatin likely reduced the Ki67 index in the present study because matuzumab blocked the cisplatin-induced activation of Erk, which is important for cancer cell proliferation as a component of the Ras-MEK-Erk signaling pathway [17,18]. The increase in the number of apoptotic cells in tumors treated with both matuzumab and cisplatin likely resulted from inhibition by matuzumab of the cisplatin-induced activation of Akt, which contributes to antiapoptotic signaling through several pathways [15,16]. Our data thus indicate that matuzumab enhanced the antitumor effect of cisplatin, with the combination treatment inhibiting tumor cell proliferation and inducing apoptosis to a greater extent than treatment with either agent alone. Our data showing that gefitinib also blocked cisplatin-induced activation of Akt and Erk may explain the previous observation that the growth-inhibitory action of cisplatin in A549 tumors was increased fourfold in combination with gefitinib [35]. Our findings suggest the importance of EGFR signaling in the development of chemoresistance to cisplatin, and they provide insight into the mechanism by which anti-EGFR mAbs might augment the efficacy of cisplatin. Clinical studies of the therapeutic efficacy of matuzumab combined with cisplatin are thus warranted.

Acknowledgments: We thank Erina Hatashita, Yuki Yamada, and Takeko Wada for technical assistance.

References

[1] Siddik, Z.H. (2003) Cisplatin: mode of cytotoxic action and molecular basis of resistance. Oncogene 22, 7265–7279.
[2] El-Abaseri, T.B., Putta, S. and Hansen, L.A. (2006) Ultraviolet irradiation induces keratinocyte proliferation and epidermal hyperplasia through the activation of the epidermal growth factor receptor. Carcinogenesis 27, 225–231.
[3] Xu, K.P., Ding, Y., Ling, J., Dong, Z. and Yu, F.S. (2004) Wound-induced HB-EGF ectodomain shedding and EGFR activation in corneal epithelial cells. Invest. Ophthalmol. Vis. Sci. 45, 813–820.
[4] King, C.R., Borrello, I., Porter, L., Comoglio, P. and Schlessinger, J. (1989) Ligand-independent tyrosine phosphorylation of EGF receptor and the erbB-2/neu proto-oncogene product is induced by hyperosmotic shock. Oncogene 4, 13–18.
[5] Chen, C.H., Cheng, T.H., Lin, H., Shih, N.L., Chen, Y.L., Chen, Y.S., Cheng, C.F., Lian, W.S., Meng, T.C., Chiu, W.T. and Chen, J.J. (2006) Reactive oxygen species generation is involved in epidermal growth factor receptor transactivation through the transient oxidization of Src homology 2-containing tyrosine phosphatase in endothelin-1 signaling pathway in rat cardiac fibroblasts. Mol. Pharmacol. 69, 1347–1355.
[6] Park, C.M., Park, M.J., Kwak, H.J., Lee, H.C., Kim, M.S., Lee, S.H., Park, I.C., Rhee, C.H. and Hong, S.I. (2006) Ionizing radiation enhances matrix metalloproteinase-2 secretion and invasion of glioma cells through Src/epidermal growth factor receptor-mediated p38/Akt and phosphatidylinositol 3-kinase/Akt signaling pathways. Cancer Res. 66, 8511–8519.
[7] Wang, F., Liu, R., Lee, S.W., Stoss, C.M., Couget, J. and Cusack, J.C. (2007) Heparin-binding EGF-like growth factor is an early response gene to chemotherapy and contributes to chemotherapy resistance. Oncogene 26, 2006–2016.
[8] Winograd-Katz, S.E. and Levitzki, A. (2006) Cisplatin induces PKB/Akt activation and p38(MAPK) phosphorylation of the EGF receptor. Oncogene 25, 7381–7390.
[9] Benhar, M., Engelberg, D. and Levitzki, A. (2002) Cisplatin-induced activation of the EGF receptor. Oncogene 21, 8723–8731.
[10] Johnson, F.M., Saigal, B. and Donato, N.J. (2005) Induction of heparin-binding EGF-like growth factor and activation of EGF receptor in imatinib mesylate-treated squamous carcinoma cells. J. Cell. Physiol. 205, 218–227.
[11] Van Schaeybroeck, S., Kyula, J., Kelly, D.M., Karaiskou-McCaul, A., Stokesberry, S.A., Van Cutsem, E., Longley, D.B. and Johnston, P.G. (2006) Chemotherapy-induced epidermal growth factor receptor activation determines response to combined gefitinib/chemotherapy treatment in non-small cell lung cancer cells. Mol. Cancer Ther. 5, 1154–1165.
[12] Carpenter, G. (1987) Receptors for epidermal growth factor and other polypeptide mitogens. Annu. Rev. Biochem. 56, 881–914.
[13] Klapper, L.N., Kirschbaum, M.H., Sela, M. and Yarden, Y. (2000) Biochemical and clinical implications of the ErbB/HER signaling network of growth factor receptors. Adv. Cancer Res. 77, 25–79.
[14] Di Marco, E., Pierce, J.H., Fleming, T.P., Kraus, M.H., Molloy, C.J., Aaronson, S.A. and Di Fiore, P.P. (1989) Autocrine interaction between TGF alpha and the EGF-receptor: quantitative requirements for induction of the malignant phenotype. Oncogene 4, 831–838.
[15] Datta, S.R., Brunet, A. and Greenberg, M.E. (1999) Cellular survival: a play in three Akts. Genes Dev. 13, 2905–2927.
[16] Goswami, A., Ranganathan, P. and Rangnekar, V.M. (2006) The phosphoinositide 3-kinase/Akt1/Par-4 axis: a cancer-selective therapeutic target. Cancer Res. 66, 2889–2892.
[17] Katz, M., Amit, I. and Yarden, Y. (2007) Regulation of MAPKs by growth factors and receptor tyrosine kinases. Biochim. Biophys. Acta 1773, 1161–1176.
[18] Roberts, P.J. and Der, C.J. (2007) Targeting the Raf-MEK-ERK mitogen-activated protein kinase cascade for the treatment of cancer. Oncogene 26, 3291–3310.
[19] Yoshida, T., Okamoto, I., Okabe, T., Iwasa, T., Satoh, T., Nishio, K., Fukuoka, M. and Nakagawa, K. (2008) Matuzumab and cetuximab activate the epidermal growth factor receptor but fail to trigger downstream signaling by Akt or Erk. Int. J. Cancer 122, 1530–1538.

[20] Okabe, T., Okamoto, I., Tamura, K., Terashima, M., Yoshida, T., Satoh, T., Takada, M., Fukuoka, M. and Nakagawa, K. (2007) Differential constitutive activation of the epidermal growth factor receptor in non-small cell lung cancer cells bearing EGFR gene mutation and amplification. Cancer Res. 67, 2046–2053.
[21] Wu, L., Birle, D.C. and Tannock, I.F. (2005) Effects of the mammalian target of rapamycin inhibitor CCI-779 used alone or with chemotherapy on human prostate cancer cells and xenografts. Cancer Res. 65, 2825–2831.
[22] Akashi, Y., Okamoto, I., Iwasa, T., Yoshida, T., Suzuki, M., Hatashita, E., Yamada, Y., Satoh, T., Fukuoka, M., Ono, K. and Nakagawa, K. (2007) The novel microtubule-interfering agent TZT-1027 enhances the anticancer effect of radiation in vitro and in vivo. Br. J. Cancer 96, 1532–1539.
[23] Higashiyama, S. and Nanba, D. (2005) ADAM-mediated ectodomain shedding of HB-EGF in receptor cross-talk. Biochim. Biophys. Acta 1751, 110–117.
[24] Miyamoto, S., Yagi, H., Yotsumoto, F., Kawarabayashi, T. and Mekada, E. (2006) Heparin-binding epidermal growth factor-like growth factor as a novel targeting molecule for cancer therapy. Cancer Sci. 97, 341–347.
[25] Ono, M., Raab, G., Lau, K., Abraham, J.A. and Klagsbrun, M. (1994) Purification and characterization of transmembrane forms of heparin-binding EGF-like growth factor. J. Biol. Chem. 269, 31315–31321.
[26] Mitamura, T., Higashiyama, S., Taniguchi, N., Klagsbrun, M. and Mekada, E. (1995) Diphtheria toxin binds to the epidermal growth factor (EGF)-like domain of human heparin-binding EGF-like growth factor/diphtheria toxin receptor and inhibits specifically its mitogenic activity. J. Biol. Chem. 270, 1015–1019.
[27] Suganuma, K., Kubota, T., Saikawa, Y., Abe, S., Otani, Y., Furukawa, T., Kumai, K., Hasegawa, H., Watanabe, M., Kitajima, M., Nakayama, H. and Okabe, H. (2003) Possible chemoresistance-related genes for gastric cancer detected by cDNA microarray. Cancer Sci. 94, 355–359.
[28] Li, S., Schmitz, K.R., Jeffrey, P.D., Wiltzius, J.J., Kussie, P. and Ferguson, K.M. (2005) Structural basis for inhibition of the epidermal growth factor receptor by cetuximab. Cancer Cell 7, 301–311.
[29] Adams, G.P. and Weiner, L.M. (2005) Monoclonal antibody therapy of cancer. Nat. Biotechnol. 23, 1147–1157.
[30] Kleespies, A., Ischenko, I., Eichhorn, M.E., Seeliger, H., Amendt, C., Mantell, O., Jauch, K.W. and Bruns, C.J. (2008) Matuzumab short-term therapy in experimental pancreatic cancer: prolonged antitumor activity in combination with gemcitabine. Clin. Cancer Res. 14, 5426–5436.
[31] Graeven, U., Kremer, B., Sudhoff, T., Killing, B., Rojo, F., Weber, D., Tillner, J., Unal, C. and Schmiegel, W. (2006) Phase I study of the humanised anti-EGFR monoclonal antibody matuzumab (EMD 72000) combined with gemcitabine in advanced pancreatic cancer. Br. J. Cancer 94, 1293–1299.
[32] Rao, S., Starling, N., Cunningham, D., Benson, M., Wotherspoon, A., Lupfert, C., Kurek, R., Oates, J., Baselga, J. and Hill, A. (2008) Phase I study of epirubicin, cisplatin and capecitabine plus matuzumab in previously untreated patients with advanced oesophagogastric cancer. Br. J. Cancer 99, 868–874.
[33] Vanhoefer, U., Tewes, M., Rojo, F., Dirsch, O., Schleucher, N., Rosen, O., Tillner, J., Kovar, A., Braun, A.H., Trarbach, T., Seeber, S., Harstrick, A. and Baselga, J. (2004) Phase I study of the humanized antiepidermal growth factor receptor monoclonal antibody EMD72000 in patients with advanced solid tumors that express the epidermal growth factor receptor. J. Clin. Oncol. 22, 175–184.
[34] Salazar, R., Tabernero, J., Rojo, F., Jimenez, E., Montaner, I., Casado, E., Sala, G., Tillner, J., Malik, R. and Baselga, J. (2004) Dose-dependent inhibition of the EGFR and signalling pathways with the anti-EGFR monoclonal antibody (MAb) EMD 72000 administered every three weeks (q3w). A phase I pharmacokinetic/pharmacodynamic (PK/PD) study to define the optimal biological dose (OBD). J. Clin. Oncol. 22 (Suppl. 14), 127.
[35] Sirotnak, F.M., Zakowski, M.F., Miller, V.A., Scher, H.I. and Kris, M.G. (2000) Efficacy of cytotoxic agents against human tumor xenografts is markedly enhanced by coadministration of ZD1839 (Iressa), an inhibitor of EGFR tyrosine kinase. Clin. Cancer Res. 6, 4885–4892.

Efficacy and Safety of Erlotinib Monotherapy for Japanese Patients with Advanced Non-small Cell Lung Cancer

A Phase II Study

Kaoru Kubota, MD, PhD, Yutaka Nishiwaki, MD, Tomohide Tamura, MD, Kazuhiko Nakagawa, MD, Kaoru Matsui, MD, Koshiro Watanabe, MD, PhD, Toyoaki Hida, MD, Masaaki Kawahara, MD, Nobuyuki Katakami, MD, Koji Takeda, MD, Akira Yokoyama, MD, Kazumasa Noda, MD, Masahiro Fukuoka, MD, and Nagahiro Saijo, MD, PhD

Introduction: The aim of this study was to evaluate the efficacy and safety of Erlotinib in Japanese patients with previously treated non-small cell lung cancer (NSCLC). Available tumor biopsy samples were analyzed to examine relationships between biomarkers and clinical outcome.

Methods: This open-label phase II trial enrolled stage III/IV NSCLC patients who had progressive disease after at least one prior platinum-based chemotherapy regimen. Erlotinib was administered at a dose of 150 mg/d orally until disease progression or intolerable toxicity. Analysis of epidermal growth factor receptor gene mutations in exon 18–21 by direct sequencing was performed in tumor tissue specimens obtained at the first diagnosis.

Results: Sixty-two patients were enrolled and 60 patients were evaluable for efficacy. Objective response rate and disease control rate were 28.3% and 50.0%; median time to progression and overall survival were 77 days and 14.7 months, respectively. In logistic regression analysis, only smoking history was proved to be a statistically significant predictive factor for response (odds ratio: 0.06, $p < 0.001$). Only 7 patients had samples available for mutation analysis. Three patients who had deletion mutations on exon 19 (del E746-A750 or del S752-I759) exhibited objective response. Common toxicities were rash (98%), dry skin (81%), and diarrhea (74%). Discontinuation due to adverse events occurred in 11 patients (18%). Four patients (6%) experienced interstitial lung disease-like events, one of whom died.

Conclusion: Erlotinib is efficacious in Japanese patients with previously treated NSCLC. The toxicity profile was similar to that in Western patients, except for a somewhat higher incidence of skin disorders and interstitial lung disease. Further studies are needed to determine the relationship between epidermal growth factor receptor mutations and outcomes with Erlotinib in Japanese patients.

National Cancer Center Hospital East, Kashiwa, Chiba, Japan.

Disclosure: Kazuhiko Nakagawa had served as an adviser for pre-approval consulting of this drug. Masahiro Fukuoka was paid an honorarium as the chairman of the meeting and as medical advisor for clinical trial in relation to this drug. Nagahiro Saijo had received research grant in relation to this drug. The other authors declare no conflicts of interest.

Address for correspondence: Kaoru Kubota, MD, PhD, National Cancer Center Hospital East, 6-5-1 Kashiwanoha, Kashiwa, Chiba 277-8577, Japan. E-mail: kkubota@east.ncc.go.jp

ISSN: 1556-0864/08/0312-1439

Key Words: Non-small cell lung cancer, Erlotinib, Molecular target therapy, EGFR-TKIs, *EGFR* mutation.

(*J Thorac Oncol.* 2008;3: 1439–1445)

Lung cancer affects approximately 1.2 million people annually, and is the leading cause of cancer death in the world.[1] More than 80% of affected patients are diagnosed with non-small cell lung cancer (NSCLC). The standard first-line treatment for metastatic NSCLC is a combination of platinum chemotherapy with a third-generation agent such as docetaxel, paclitaxel, gemcitabine, vinorelbine, and irinotecan.[2,3] Although patients with stage II, IIIA, or IIIB NSCLC receive platinum-based chemotherapy as part of combined modality treatment with thoracic radiotherapy or surgery, many will be candidates for second or third-line chemotherapy. Docetaxel is the only cytotoxic agent with a proven survival advantage over supportive care in patients with disease progression after cisplatin-based chemotherapy for NSCLC.[4] The other agent for which a survival benefit has been demonstrated in this setting is erlotinib,[5] which was approved in Japan for the treatment of relapsed NSCLC in October 2007. Erlotinib is a selective, orally active epidermal growth factor receptor tyrosine kinase inhibitor (EGFR-TKI). In contrast to the experience with the cytotoxic chemotherapeutic agents, response to treatment with EGFR-TKIs has been reported to be influenced by gender, histological type, race or ethnic origin, and smoking status.[5–8]

Tumor molecular markers, including *EGFR* gene mutations and protein expression, have been widely studied in patients with NSCLC, and there is strong evidence that the presence of *EGFR* gene mutations is a predictor of tumor response and resistance.[9–12] However, few prospective studies have evaluated molecular markers as predictors of outcome, and their clinical usefulness is unproven.

This report presents the results of the first phase II study of erlotinib conducted in Japanese patients with NSCLC. The purpose was to evaluate the efficacy and safety of erlotinib in this population. Where available, tumor biopsy samples were analyzed for EFGR-related markers.

PATIENTS AND METHODS

This phase II, multicenter, open-label study recruited patients at 11 hospitals in Japan. The primary end point was the objective response rate (ORR) to erlotinib treatment (150 mg/d). Secondary endpoints were disease control rate (DCR), response duration, time to progression, overall survival (OS), quality of life (QoL), and safety. The protocol was approved by the ethics review boards of all participating institutions, and conducted in accordance with Japanese Good Clinical Practice guidelines.

Patient Selection

Patients with histologically or cytologically documented stage IIIB or IV NSCLC at study entry (not curable with surgery or radiotherapy) that was recurrent or refractory to treatment with one or more chemotherapy regimens (including at least one platinum-containing regimen), were enrolled into this study. Additional eligibility criteria included: the presence of measurable lesions by Response Evaluation Criteria in Solid Tumors (RECIST); age $\geq$20, $<$75 years; Eastern Cooperative Oncology Group performance status (ECOG PS) of 0–2, and adequate bone marrow, hepatic, and renal function, i.e., aspartate aminotransferase and alanine aminotransferase (ALT) levels $\leq$2.5 times the upper limit of normal and total bilirubin of $\leq$1.5 times the upper limit of normal. Patients with existing or previous interstitial lung disease (ILD) were excluded, although a history of radiation pneumonitis (limited to the field of radiation treatment) was permitted. Concomitant anticancer treatment and prophylactic medication for adverse events (AEs) were not permitted, nor was prior use of anti-EGFR or anti human epidermal growth factor receptor (HER2) agents (small molecules and monoclonal antibodies). Written informed consent was obtained from all patients.

Treatment Procedure

After completion of the baseline assessments (see below), all patients received erlotinib (150 mg orally) each morning, 1 hour before breakfast, until the occurrence of progressive disease (PD) or unacceptable toxicity (all AEs were graded using the National Cancer Institute Common Toxicity Criteria Version 2.0). In the event of treatment-related toxicity, 2 dose reductions of 50 mg were permitted per patient, and dosing could also be interrupted for up to 14 days. For grade 3 or intolerable grade 2 rash, treatment was withheld until the rash improved to grade 2 or less, when a lower dose of erlotinib was initiated. For grade 3 diarrhea, treatment was withheld until the diarrhea was grade 1 or less, when a lower dose was started. For ILD of any grade, or any grade 4 toxicity, treatment was immediately and permanently discontinued.

Evaluation of Efficacy

Objective tumor response was assessed in accordance with RECIST.[13] Tumor assessments were performed at baseline, then every 4 weeks until week 16, and then every 8 weeks thereafter. Confirmation of complete or partial responses (PR) was required, by means of a second assessment conducted 28 days or more after the initial assessment. Stable disease (SD) was defined as disease control (absence of progression) maintained for at least 6 weeks. An independent response evaluation committee consisting of 2 oncologists and a radiologist reviewed images of patients with complete response, PR, and SD. Individual survival times were determined from the survival status of each patient during the study period and at the post study follow-up survey conducted in June-July 2005 and May-July 2006. OS was defined as the time from first administrated to death.

Quality of Life Evaluation

The Functional Assessment of Cancer Therapy-Lung (FACT-L) questionnaire (Version 4-A)[14] was used to assess QoL. The full FACT-L questionnaire was administered at baseline and then every 28 days. In addition, the Lung Cancer Subscale (LCS), an independently validated component of FACT-L, was administered weekly during the treatment period. Best responses on the LCS were analyzed for all patients with a baseline LCS score of 24 or less (out of a possible 28 points) and symptomatic improvement was defined as an increase from the baseline score of 2 or more points, sustained for at least 4 weeks.

Evaluation of Safety

Baseline assessment included a full patient history, physical examination, standard laboratory tests, electrocardiography, chest radiography, pregnancy test, and ophthalmologic tests (vision test and slit-lamp examination). Every week until week 8 and every 2 weeks thereafter, vital signs and ECOG PS were monitored and blood samples were taken for hematology and blood chemistry tests. A radiograph examination to assess pulmonary toxicity was conducted weekly until week 4 and every 2 weeks thereafter. Ophthalmologic examinations were repeated at week 8 and at the end of the study. Observation and evaluation of AEs was conducted as appropriate throughout the study period. All AEs were graded using National Cancer Institute Common Toxicity Criteria Version 2.0. For all ILD-like events, the data safety monitoring board (which consisted of oncologists and pneumonologists) reviewed the clinical data and images; the images were also examined by a review committee of radiologists with expertise in drug-induced pulmonary disorders.

Biomarker Analysis

EGFR mutations and EGFR and HER2 protein expression were assessed in patients with suitable tumor tissue specimens at first diagnosis or surgery; these assessments were done only with separate written consent. Tumor samples were obtained from each center as formalin-fixed and paraffin-embedded blocks, or as thinly sliced tissue sections mounted on glass microscope slides. For the mutation analysis, the tissue was microdissected by Targos Molecular Pathology (Kassel, Germany) and direct sequencing was conducted at the Roche Centre of Medical Genomics (Basel, Switzerland), using a nested polymerase chain reaction of exon 18–21. EGFR protein expression was analyzed by Lab Corp (Mechelen, Belgium). EGFR expression analysis was conducted by immunohistochemistry using Dako EGFR PharmDx™ kits (Dako, Carpinteria, CA). A positive test was

defined as membranous staining in ≥10% of the tumor cells. HER2 protein expression was measured using HercepTest™ (Dako, Carpinteria, CA), and a score of 1+ or above (possible scores were: 0, 1+, 2+, 3+) was regarded as positive.

Statistical Analysis

Given an expected ORR of 20%, a Fisher's exact test was performed (one-sided $\alpha = 2.5\%$). Based on 50 patients, the power to test the null hypothesis (ORR = 5%) was 89.66%. The target sample size of 60 patients was chosen on the expectation that a proportion of patients would prove to be ineligible for the study. The main analysis of efficacy was conducted on the full analysis set (FAS), which was produced by omitting ineligible patients. The 95% confidence interval (CI) for ORR, DCR, and symptom improvement rate was calculated by the Clopper-Pearson method. The time-to-event variables were estimated by the Kaplan-Meier method. Logistic regression and Cox proportional hazards regression analysis was conducted on best response and survival time, respectively. In both cases, univariate and multivariate analyses were used to evaluate the effects of 11 factors relating to patient and disease characteristics, and previous treatment.

RESULTS

Patient Characteristics

A total of 62 patients were enrolled between December 2003 and January 2005. All were evaluable for safety and 60 were evaluable for efficacy (FAS). Two patients did not have a measurable lesion according to RECIST. The baseline characteristics of the patients, including their treatment history, are shown in Table 1. The median age was 60.5 years (range: 28–74 years), and 71% of patients were male. Fifty-seven patients (92%) had adenocarcinoma, and 20 (32%) were never-smokers. Twenty-seven patients (44%) had received only one previous chemotherapy regimen.

Efficacy

Tumor response rates in the FAS (as assessed by extrainstitutional review) are shown in Table 2. Seventeen patients were assessed as having a PR and 13 as having SD. The ORR was 28.3% (95% CI: 17.5–41.4%) and the DCR was 50% (95% CI: 36.8–63.2%). In three patients, objective response could not be adequately confirmed, because each discontinued treatment early in the study due to AEs. The median duration of response was 278 days (95% CI: 203–422 days), and time to progression was 77 days (95% CI: 55–166 days). OS was determined based on information collected until the follow-up survey conducted in May–July 2006. The median survival time was 14.72 months (95% CI: 11.07–20.57 months; 19 censored cases) and the 1-year survival rate was 56.5% (95% CI: 43.9–69.1%) (Figure 1). The median OS of patients with PD was 9.95 months. The symptom improvement rate measured using the LCS was 42.1% (24/57; 95% CI: 29.1–55.9%).

The overall response rate was higher in women (58.8%; 10/17) than in men (16.3%; 7/43, χ^2 test: $p = 0.0029$), and in never-smokers (63.2%; 12/19) than in current or former smokers (12.2%; 5/41, $p = 0.0002$). There was no statistically significant difference between the response rate in patients with adenocarcinoma (28.6%; 16/56) and nonadenocarcinoma histology (25.0%; 1/4, $p = 1.0000$). The response

TABLE 1. Summary of Baseline Patient Characteristics and Demographics

Patient and Disease characteristics	No. of Patients ($n = 62$)	%
Age (yr)		
Median	60.5	
Range	28–74	
Sex		
Female	18	29
Male	44	71
Performance status		
0	20	32
1	41	66
2	1	2
Histology		
Adenocarcinoma	57	92
Squamous cell	4	6
Unclassified	1	2
Stage		
IIIB	8	13
IV	54	87
Smoking history		
Never smoked	20	32
Current- or former smoker	42	68
Time since initial diagnosis (d)		
Median	304.0	
Range	2–2353	
Prior chemotherapy regimens		
1	27	44
2	23	37
≥3	12	19
Prior taxanes		
No	10	16
Yes	52	84
Time since last regimen (d)		
Median	80.0	
Range	29–528	

TABLE 2. Response Assessment

Parameter	n	(%)
Partial response	17	28.3
Stable disease	13	21.7
Progressive disease	27	45.0
Not assessable	3	5.0
Response rate (%) (95% CI)	28.3 (17.5–41.4)	
Disease control rate (%) (95% CI)	50.0 (36.8–63.2)	
Duration of response (median: days)[a] (95% CI)	278 (203.0–422.0)	
Time to progression (median: days)[a] (95% CI)	77 (55–166)	

[a] Kaplan-Meier method.
CI, confidence intervals.

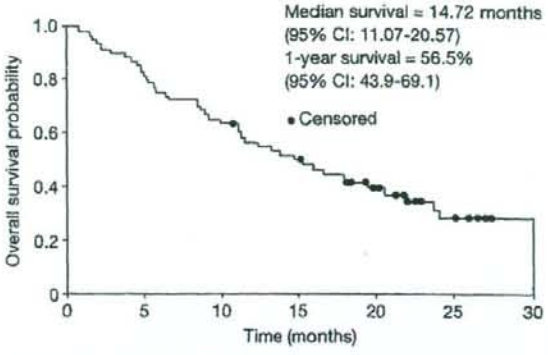

FIGURE 1. Kaplan-Meier plot showing overall survival.

rate was not affected by the number of previous chemotherapy regimens, however, being 27% for patients with one previous regimen (7/26) and 29% for those with 2 or more regimens (10/34). No statistically significant differences were found between other patient subgroups. In a multivariate logistic regression analysis, only smoking history was found to be a statistically significant predictor of response. A multivariate Cox regression analysis showed that both smoking history and ECOG PS were significant predictors for OS (Table 3).

Safety

All 62 patients who received erlotinib were assessed for safety. Treatment-related AEs were observed in all patients, and there were 24 serious AEs in 18 patients (29%). AEs led to discontinuation of erlotinib in 11 patients (18%), including 3 due to ILD-like events, 2 due to ALT elevation, and one each due to rash, paronychia, punctate keratitis, dyspnea/hypoxia, pneumonia and fever/inflammatory neck swelling, and to dose interruptions in 30 patients (48.4%). While the main reasons for the dose interruptions were rash (n = 15; 24.2%) and diarrhea (n = 4; 6.5%), only one patient with rash

TABLE 3. Logistic and Cox Regression Analysis

	Odds Ratio[b]	(95% CI)	p
Logistic regression analysis of response			
Univariate analysis			
Sex (female vs male)	0.14	0.04–0.48	0.002
Age (<65 vs ≥65)	1.26	0.38–4.13	0.704
Histology (non-AD vs AD)	1.20	0.12–12.41	0.878
Smoking history (never vs current or former)	0.08	0.02–0.30	<0.001
Performance status (0 vs ≥1)	0.62	0.19–1.98	0.420
Prior regimens (1 vs ≥2)	1.13	0.36–3.53	0.832
Stage (IIIB vs IV)	0.99	0.17–5.65	0.988
KL-6 (baseline) (<median [496.5 U/ml[a]] vs ≥median)	1.64	0.53–5.12	0.392
Best response to previous chemotherapy (non-PR vs PR)	0.90	0.24–3.33	0.869
Prior taxanes (no vs yes)	0.43	0.10–1.84	0.253
Time since initial diagnosis (≤12 mo vs >12 mo)	1.02	0.31–3.30	0.976
Multivariate analysis			
Smoking history (never vs current or former)	0.06	0.02–0.28	<0.001
Time since initial diagnosis (<12 mo vs ≥12 mo)	2.22	0.49–10.20	0.304
Cox regression analysis of survival			
Univariate analysis			
Sex (female vs male)	1.76	0.85–3.61	0.126
Age (<65 vs ≥65)	0.86	0.44–1.71	0.675
Histology (non-AD vs AD)	0.55	0.19–1.55	0.255
Smoking history (never vs current or former)	1.90	0.93–3.90	0.079
Performance status (0 vs ≥1)	2.31	1.12–4.73	0.023
Prior regimens (1 vs ≥2)	0.93	0.50–1.75	0.833
Stage (IIIB vs IV)	1.38	0.49–3.89	0.542
KL-6 (baseline) (<median [496.5 U/ml[a]] vs ≥median)	1.64	0.87–3.06	0.125
Best response to previous chemotherapy (non-PR vs PR)	0.66	0.31–1.44	0.300
Prior taxanes (no vs yes)	2.09	0.74–5.90	0.163
Time since initial diagnosis (≤12 mo vs >12 mo)	0.76	0.40–1.47	0.418
Multivariate analysis			
Smoking history (never vs current or former)	2.20	1.06–4.56	0.035
Performance status (0 vs ≥1)	2.59	1.25–5.37	0.011

[a] Or 629 ng/ml.
[b] Left site of 'vs' indicates reference group.
PR, partial response; AD, adenocarcinoma; CI, confidence interval.

TABLE 4. Major Treatment-Related Adverse Events and Interstitial Lung Disease-Like Events

			NCI-CTC Grade (*n*)			
Event[a]	*n*	%	1	2	3	>4
Rash	61	98.4	18	41	2	0
Dry skin	50	80.6	44	6	—	—
Diarrhea	46	74.2	33	10	3	0
Pruritus	45	72.6	38	7	0	—
Stomatitis	24	38.7	19	4	1	0
Fatigue	21	33.9	15	6	0	0
Anorexia	19	30.6	11	6	2	0
Paronychia	18	29.0	12	5	1	0
C-reactive protein increased	15	24.2	8	7	0	0
Alanine aminotransferase increased	15	24.2	11	2	2	0
Total bilirubin increased	15	24.2	8	7	0	0
Weight loss	13	21.0	13	0	0	—
ILD-like events	4	6.5	1	0	2	1[b]

Case	Sex	Age	Smoking History	Brinkman Index	Performance Status	Histology	Onset (day)	Outcome	Relation to Erlotinib[c]
1	Male	75	Former	640	1	Adenocarcinoma	52	Recovery	Probable
2	Male	67	Never	—	1	Adenocarcinoma	103	Death (145)	Possible
3	Female	39	Never	—	0	Adenocarcinoma	85	Recovery	Probable
4	Male	69	Former	1000	1	Adenocarcinoma	13	Recovery	Unlikely

[a] Categorized by MedDra Ver.7.1 (except for event).
[b] Grade 5.
[c] Judged by ILD review committee.
NCI-CTC, National Cancer Institute Common Toxicity Criteria; ILD, interstitial lung disease.

had to discontinue treatment, and no patients had to discontinue because of diarrhea or any other digestive toxicity. Fourteen patients (23%) had dose reductions due to AEs, mostly due to rash ($n = 9$; 15%). Treatment-related AEs with an incidence of 20% or more are shown in Table 4; the main events were rash (98%), dry skin (81%), and diarrhea (74%). Elevated laboratory test values related to liver function were found in some patients (total bilirubin: 24%, ALT: 24%), and grade 3 ALT elevation led to treatment discontinuation in 2 patients. Four patients had ILD-like events, including worsening of radiation pneumonitis in one patient, and one died (Table 4). All four (three men; one woman) had an ECOG PS of 0–1 and 2 were former smokers. The patient who died was a 67-year-old man with adenocarcinoma and no history of smoking who discontinued treatment on day 84 due to PD. He developed interstitial pneumonia on day 103 and received 3 days of palliative thoracic irradiation from day 99, after completing the study (3 Gy × 3 days). A computed tomography scan showed characteristic features of ILD (cryptogenic organizing pneumonia-like pattern), and the ILD review committee decided that use of erlotinib could not be excluded as the cause. For the patient with worsening of radiation pneumonitis (case 4), the committee concluded that there was a possible influence of previous radiation therapy, and that this could be seen in the computed tomography scan on day 1. There was, therefore, little reason to suspect that the use of erlotinib had been the cause. Rather, it appeared that the radiation pneumonitis had worsened according to the normal course of illness.

Biomarker Analysis

Tissue samples for measurement of *EGFR* mutations were available for 16 of the 60 patients evaluated for efficacy. For 7 patients, all base sequences were successfully identified in the 4 segments of exons 18–21. All seven (three men, four women) had adenocarcinoma; three were never-smokers, three former smokers and one a current smoker. Three had PR, two SD and two PD. Five of the seven patients had *EGFR* gene mutations and, in all, seven different mutations were detected. The 3 patients with PR all had deletion mutations in exon 19 (del E746-A750 or del S752-I759). One of the 2 patients with PD had no mutations and the other had 2 substitution mutations: L858R in exon 21 and the resistance mutation T790M in exon 20 (Table 5).

Paraffin-embedded tissue samples for immunohistochemistry were available from 12 patients, among whom, 11 had successful determinations of immunohistochemical staining (including 3 patients with PR). Six of the 11 were found to be EGFR-positive and 4 were HER2-positive. However, there were no notable relationships between the EGFR and HER2 expression status and either tumor response or patient characteristics such as sex, histological type or smoking history (data not shown).

DISCUSSION

The present study was conducted on the basis of results from a phase I study of erlotinib in Japanese patients with solid tumors,[15] which showed erlotinib to be well tolerated at

TABLE 5. *EGFR* Mutation Analysis

Response	TTP (d)	Survival (d)	Sex	Histology	Smoking history	Mutation status	Exon	Type of Mutation
PR	222	546	Female	Adenocarcinoma	Never	+	19	del E746–A750
PR	230	811+	Male	Adenocarcinoma	Current	+	19	del S752 –I759 and T751N
PR	278+	911	Female	Adenocarcinoma	Never	+	19	V786M, del E746–A750
SD	224	649+	Male	Adenocarcinoma	Former	+	21	del V834-
SD	77	737	Female	Adenocarcinoma	Former	–	—	—
PD	60	604+	Female	Adenocarcinoma	Never	+	20, 21	L858R, T790M
PD	19	347	Male	Adenocarcinoma	Former	–	—	—

TTP, time to progression; PR, partial response; SD, stable disease; PD, progressive disease.

a dose of 150 mg/d, as well as a phase II study of erlotinib in NSCLC conducted in the United States.[16] In this study, erlotinib achieved an ORR of 28.3%, which was higher than expected, and a DCR of 50%. The response rate was higher than that determined in the above-mentioned phase II study[16] and in keeping with the rate seen in the Japanese subgroup in the phase II study of gefitinib (IDEAL1; 27.5%).[6] Assessment of QoL using the LCS demonstrated a clinically meaningful rate of symptom improvement of 42.1%.

The characteristics of the patients in this study were generally similar to those of NSCLC patients as a whole, in terms of their demographics and disease and treatment history, with the exception of a particularly high proportion of patients with adenocarcinoma (92%). The possibility of enrollment bias on the basis of histological type cannot be ruled out, in part because enrollment coincided with the emergence of reports that the efficacy of EGFR-TKI therapy was greater in patients with adenocarcinoma.[17] However, we also observed one PR and two SDs among three patients with squamous cell carcinoma (FAS population), and our results do not rule out the efficacy of erlotinib in any patient subtype. A multivariate logistic regression analysis showed that smoking status was significantly associated with tumor response, in agreement with previous studies of predictive factors for response to EGFR-TKIs.[5,18,19]

The median survival time with erlotinib was an encouraging 14.7 months. One of the reasons for this long survival may be the high proportion of never-smokers and patients with adenocarcinoma compared with those of other studies, particularly the multinational phase III erlotinib study (BR.21).[5] On the other hand, the presence of *EGFR* gene mutations is currently regarded as an important determinant of treatment response to EGFR-TKIs[20,21] and may be the most important factor in relation to the favorable results seen in the present study. However, it is important to recognize that the potential prognostic effect of mutation status cannot be excluded. The sample size of this and previous trials limits the interpretation of this effect, which will be adequately assessed only by means of appropriately powered trials specifically designed to examine these factors.

Assessment of the presence or absence of *EGFR* gene mutation was possible in only seven patients in the present study. Despite this, the results were consistent with the results of some previous studies. All three of the patients who had a PR (including a male current smoker) had an in-frame deletion in exon 19, which is considered to be the most frequent mutation site in the EGFR-TK domain.[22] One of the 2 patients with PD had a point substitution mutation (L858R) in exon 21, the second most frequent mutation site,[22] and a point mutation (T790M) in exon 20, which is suggested to be involved in tolerance to EGFR-TKI.[12,23,24] It would be valuable to conduct further prospective randomized studies on the association between these markers and survival during treatment with erlotinib in Japanese patients.

Rash and diarrhea were the main AEs reported by patients on erlotinib treatment, as reported in previous studies.[5,15,16] Rash was observed in almost all patients, and was the main reason for treatment interruptions or dose reductions. Although the protocol allowed treatment to be interrupted for grade 3 rash (or intolerable grade 2 rash), grade 3 rash only occurred in 2 patients, leading to discontinuation of treatment in one. Most cases of rash responded to symptomatic treatment and either interruption or dose reduction of erlotinib. Despite suggestions in some reports that the presence of erlotinib-related rash is associated with treatment efficacy and can be used to predict response,[25] no supportive evidence was found in the present study.

The incidence of ILD, which is the most clinically problematic AE associated with erlotinib, tended to be higher than that reported in other clinical studies of erlotinib.[5,26] This is in keeping with this class of agent, and is not unexpected in the Japanese population.

We would recommend that careful screening of patients for ILD risk factors, particularly signs of interstitial pneumonia and pulmonary fibrosis, is done before erlotinib therapy is initiated. Individuals with any previous history of ILD were excluded from this study.

In conclusion, erlotinib (150 mg/d) was shown to have promising antitumor efficacy in Japanese patients with previously treated NSCLC, leading to clinically meaningful improvements in symptoms and an encouraging median survival time. Despite, as expected, a high rate of rash and diarrhea, erlotinib was well tolerated at a dose of 150 mg/d by the majority of patients.

REFERENCES

1. Parkin MD. Global cancer statistics in the year 2000. *Lancet Oncol* 2001;2:533–543.
2. Schiller JH, Harrington D, Belani CP, et al. Comparison of four chemotherapy regimens for advanced non-small cell lung cancer. *N Engl J Med* 2002;346:92–98.

3. Ohe Y, Ohashi Y, Kubota K, et al. Randomized phase III study of cisplatin plus irinotecan versus carboplatin plus paclitaxel, cisplatin plus gemcitabine, and cisplatin plus vinorelbine for advanced non-small-cell lung cancer: four-arm cooperative study in Japan. *Ann Oncol* 2007;18: 317–323.
4. Shepherd FA, Dancey J, Ramlau R, et al. Prospective randomized trial of docetaxel versus best supportive care in patients with non-small cell lung cancer previously treated with platinum-based chemotherapy. *J Clin Oncol* 2000;18:2095–2103.
5. Shepherd F, Rodrigues J, Ciuleanu T, et al. Erlotinib in previously treated non-small cell lung cancer. *N Engl J Med* 2005;353:123–132.
6. Fukuoka M, Yano S, Giaccone G, et al. Multi-institutional randomized phase II trial of gefitinib for previously treated patients with advanced non-small-cell lung cancer. *J Clin Oncol* 2003;21:2237–2246.
7. Chang A, Parikh P, Thongprasert S, et al. Gefitinib (IRESSA) in patients of Asian origin with refractory advanced non-small cell lung cancer: subset analysis from the ISEL study. *J Thorac Oncol* 2006;1:847–855.
8. Miller VA, Kris MG, Shah N, et al. Bronchioloalveolar pathologic subtype and smoking history predict sensitivity to gefitinib in advanced non-small-cell lung cancer. *J Clin Oncol* 2004;22:1103–1109.
9. Paez JG, Jänne PA, Lee JC, et al. EGFR mutations in lung cancer: correlation with clinical response to gefitinib therapy. *Science* 2004;304: 1497–1500.
10. Lynch TJ, Bell DW, Sordella R, et al. Activating mutations in the epidermal growth factor receptor underlying responsiveness of non-small-cell lung cancer to gefitinib. *N Engl J Med* 2004;350:2129–2139.
11. Kobayashi S, Boggon TJ, Dayaram T, et al. EGFR mutation and resistance of non-small-cell lung cancer to gefitinib. *N Engl J Med* 2005;352:786–792.
12. Pao W, Miller V, Zakovski M, et al. EGF receptor gene mutations are common in lung cancers from "never smokers" and are associated with sensitivity of tumors to gefitinib and erlotinib. *Proc Natl Acad Sci USA* 2004;101:13306–13311.
13. Therasse P, Arbuck SG, Eisenhauer EA, et al. New guidelines to evaluate the response to treatment in solid tumors. *J Natl Cancer Inst* 2000;92:205–216.
14. Cella DF, Bonomi AE, Lloyd SR, et al. Reliability and validity of the functional assessment of cancer therapy-lung (FACT-L) quality of life instrument. *Lung Cancer* 1995;12:199–220.
15. Yamamoto N, Horiike A, Fujisaka Y, et al. Phase I dose-finding and pharmacokinetic study of the oral epidermal growth factor receptor tyrosine kinase inhibitor Ro50–8231 (erlotinib) in Japanese patients with solid tumors. *Cancer Chemother Pharmacol* 2008;61:489–496.
16. Pérez-Soler RS, Chachoua A, Hammond LA, et al. Determinants of tumor response and survival with erlotinib in patients with non-small-cell lung cancer. *J Clin Oncol* 2004;22:3238–3247.
17. Kaneda H, Tamura K, Kurata T, et al. Retrospective analysis of the predictive factors associated with the response and survival benefit of gefitinib in patients with advanced non-small-cell lung cancer. *Lung Cancer* 2004;46:247–254.
18. Thatcher N, Chang A, Parikh P, et al. Gefitinib plus best supportive care in previously treated patients with refractory advanced non-small cell lung cancer: results from a randomised, placebo-controlled, multicentre study (Iressa Survival Evaluation in Lung Cancer). *Lancet* 2005;366: 1527–1537.
19. Clark GM, Zborowski DM, Santabárbara P, et al. Smoking history and epidermal growth factor receptor expression as predictors of survival benefit from erlotinib for patients with non-small-cell lung cancer in the National Cancer Institute of Canada Clinical Trials Group study BR. 21. *Clin Lung Cancer* 2006;7:389–394.
20. Toyooka S, Matsuo K, Shigematsu H, et al. The impact of sex and smoking status on the mutational spectrum of epidermal growth factor receptor gene in non small cell lung cancer. *Clin Cancer Res* 2007;13: 5763–5768.
21. Mitsudomi T, Kosaka T, Endoh H, et al. Mutations of the epidermal growth factor receptor gene predict prolonged survival after gefitinib treatment in patients with non-small cell lung cancer with postoperative recurrence. *J Clin Oncol* 2005;23:2513–2520.
22. Sequist LV, Bell DW, Lynch TJ, et al. Molecular predictors of response to epidermal growth factor receptor antagonists in non-small-cell lung cancer. *J Clin Oncol* 2007;25:587–595.
23. Pao W, Miller VA, Politi KA, et al. Acquired resistance of lung adenocarcinomas to gefitinib or erlotinib is associated with a second mutation in the EGFR kinase domain. *PLoS Med* 2005;2:e73.
24. Tokumo M, Toyooka S, Ichihara S, et al. Double mutation and gene copy number of EGFR in gefitinib refractory non-small cell lung cancer. *Lung Cancer* 2006;53:117–121.
25. Wacker B, Nagrani T, Weinberg J, et al. Correlation between development of rash and efficacy in patients treated with the epidermal growth factor receptor tyrosine kinase inhibitor erlotinib in two large phase III studies. *Clin Cancer Res* 2007;13:3913–3921.
26. Tsuboi M, Le Chevalier T. Interstitial lung disease in patients with non-small cell lung cancer treated with epidermal growth factor receptor inhibitors. *Med Oncol* 2006;23:161–170.